

Thermoacoustic generation in graphene field-effect transistors

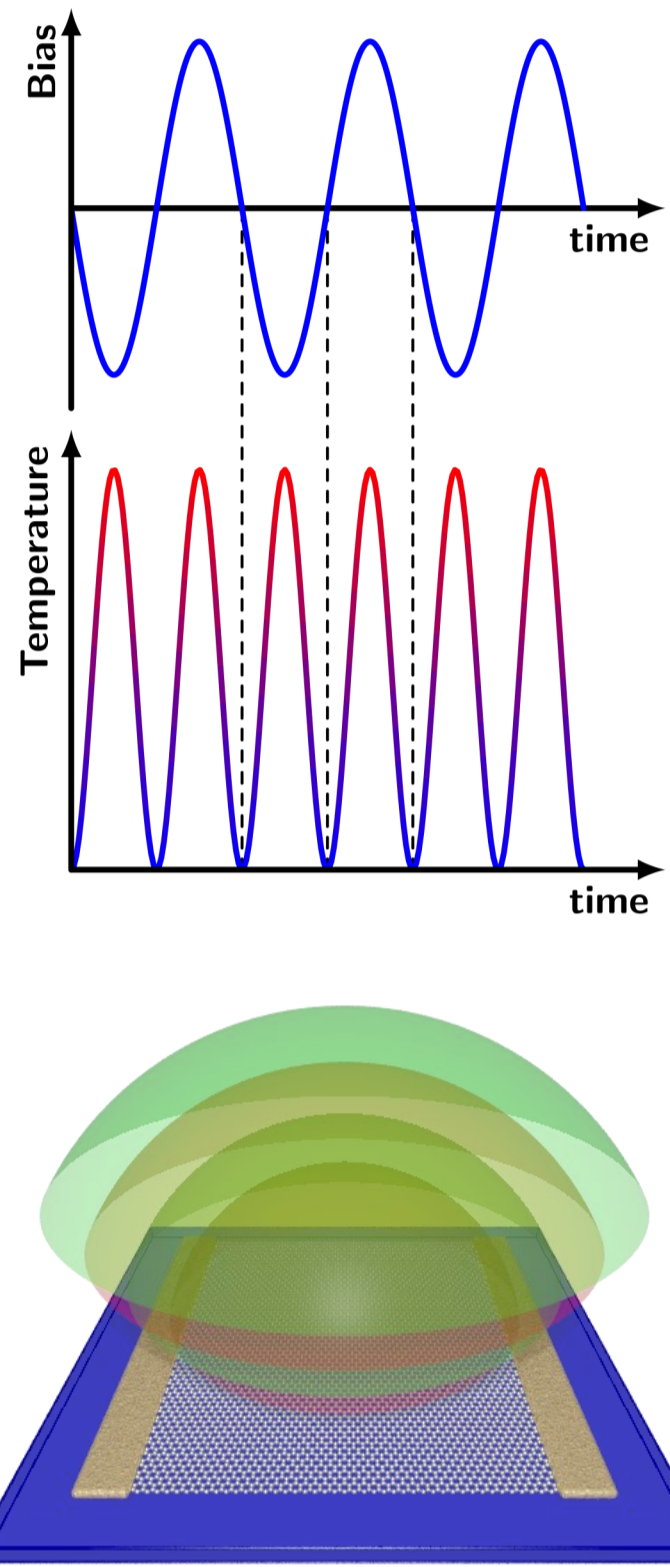


Mark S. Heath* and David W. Horsell
School of Physics and Astronomy, University of Exeter, UK
*M.Heath@exeter.ac.uk



Graphene is an ideal material for thermoacoustic generation where modulated heating of the crystal is converted directly into an acoustic signal in the surrounding media. In a graphene field-effect transistor (FET), this modulation can occur in response to an electrical current driven through the channel and voltage applied to the gate. We show that control of the charge transport in back- and top-gated FETs in air can influence the magnitude, phase and harmonic content of the sound. In particular, we show that the gate voltage can be used to tune this output sound power by over an order of magnitude.

1. Introduction



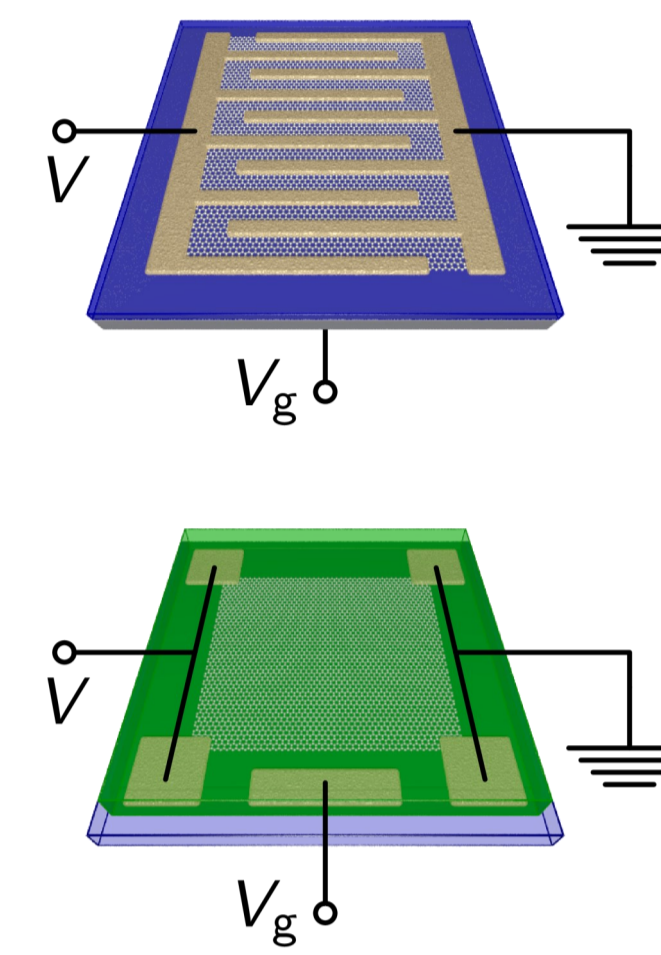
- The **thermoacoustic effect** is the transduction of heat into sound. Here, Joule heating of graphene [1] by an ac bias, V_a at frequency f produces an acoustic response at the second harmonic, $2f$.
- Graphene** is a very effective thermoacoustic material [2,3] due to a combination of high thermal conductivity, κ , low specific heat capacity, c , and atomic scale thickness, d .
- In air (a) on a substrate (s), graphene (g) produces sound with pressure [4]

$$\delta p = \frac{3}{4\pi v_a^2} \left(\frac{e_a}{e_a + e_s + e_g^*} \right) \frac{fP}{r} \quad (1)$$

where r is the distance from the source, v_a is the velocity of sound in air, $P = GV^2$, G is the conductance, ρ is the density and

$$e_{a(s)} = \left(\kappa_{a(s)} \rho_{a(s)} c_{a(s)} \right)^{1/2} \quad e_g^* = (2\pi f d \rho c)^{1/2}$$

2. Methods

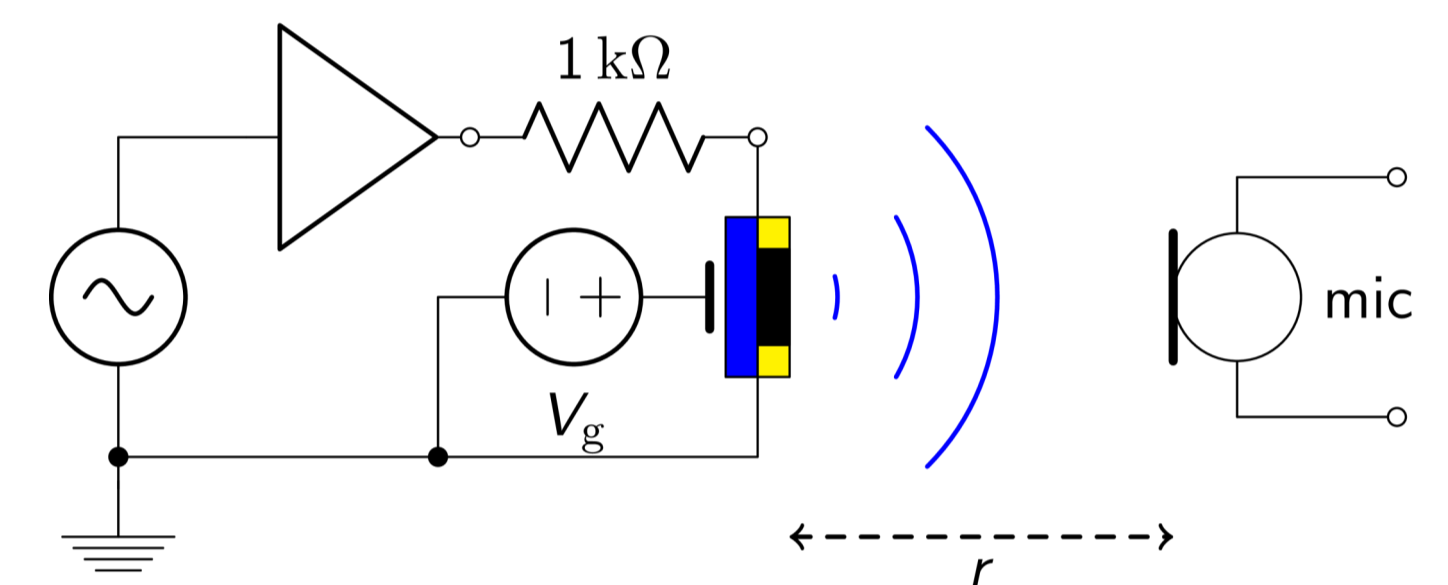


Device Fabrication

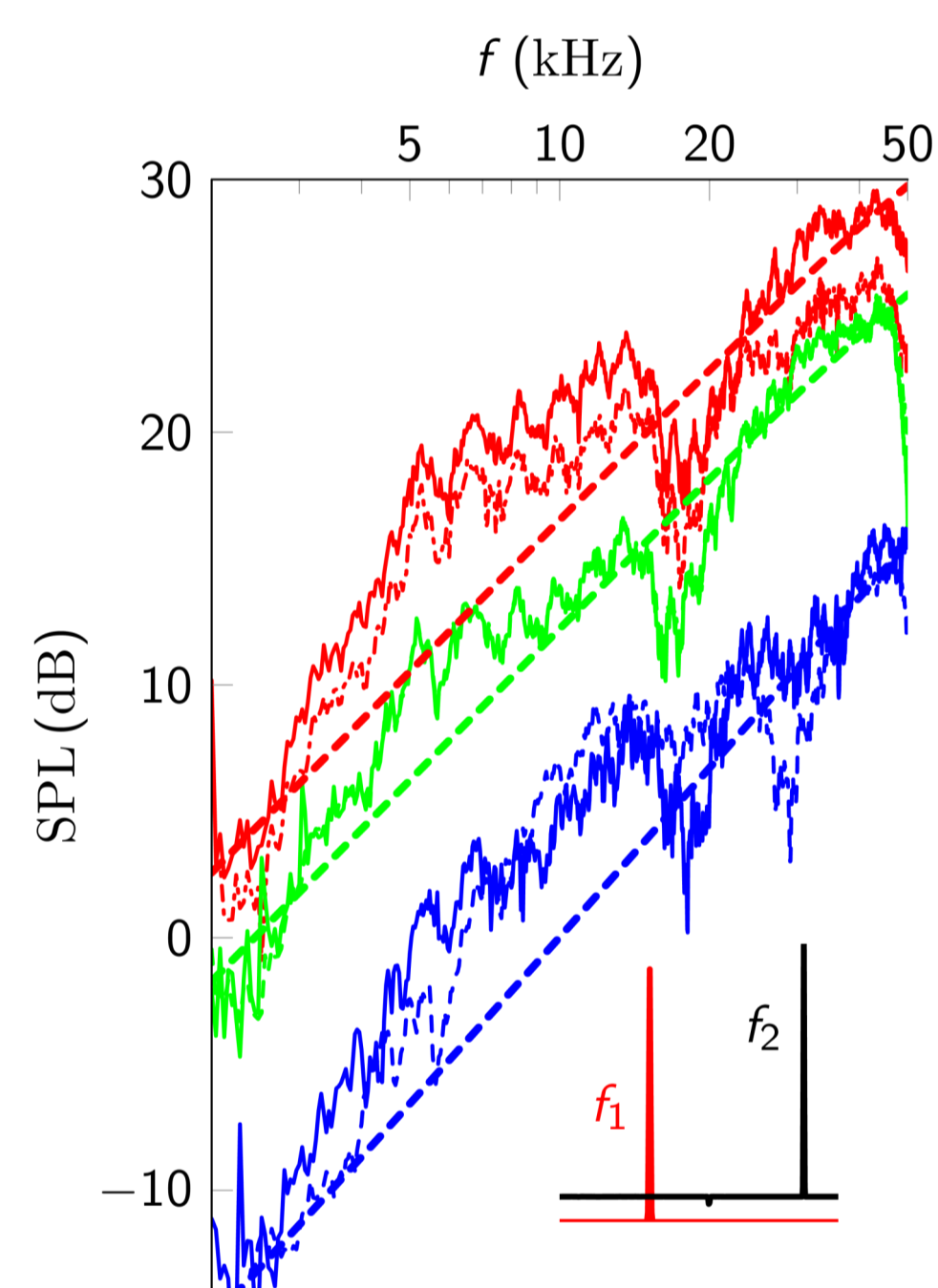
- CVD grown monolayer graphene on substrate etched into 6mm² squares using reactive ion etching (oxygen/argon).
- Contacts defined using e-beam lithography or shadow-masks.
- Two-stage contacts formed using thermal evaporation. Au on graphene and then overlap contact of Cr/Au on substrate.
- Contacts contributed <3% to device resistance.
- Back-gated FETs formed on SiO₂(300 nm)/p⁺Si substrates.
- Top-gated FETs formed on quartz substrates with a LiClO₄/PEO polymer layer drop-cast on the graphene.

Sound Measurements

- Measurements made using a lock-in amplifier and a calibrated condenser microphone.
- Device-microphone separation varied from 5 mm to 2 m.



3. Results



Thermoacoustic response spectra

Sound pressure level (SPL) as a function of frequency. The SPL is the measured sound pressure at 1m distance relative to a reference pressure of 20 μ Pa. (0 dB is the limit of human hearing at 1m at $f=1$ kHz.) $P=1$ W.

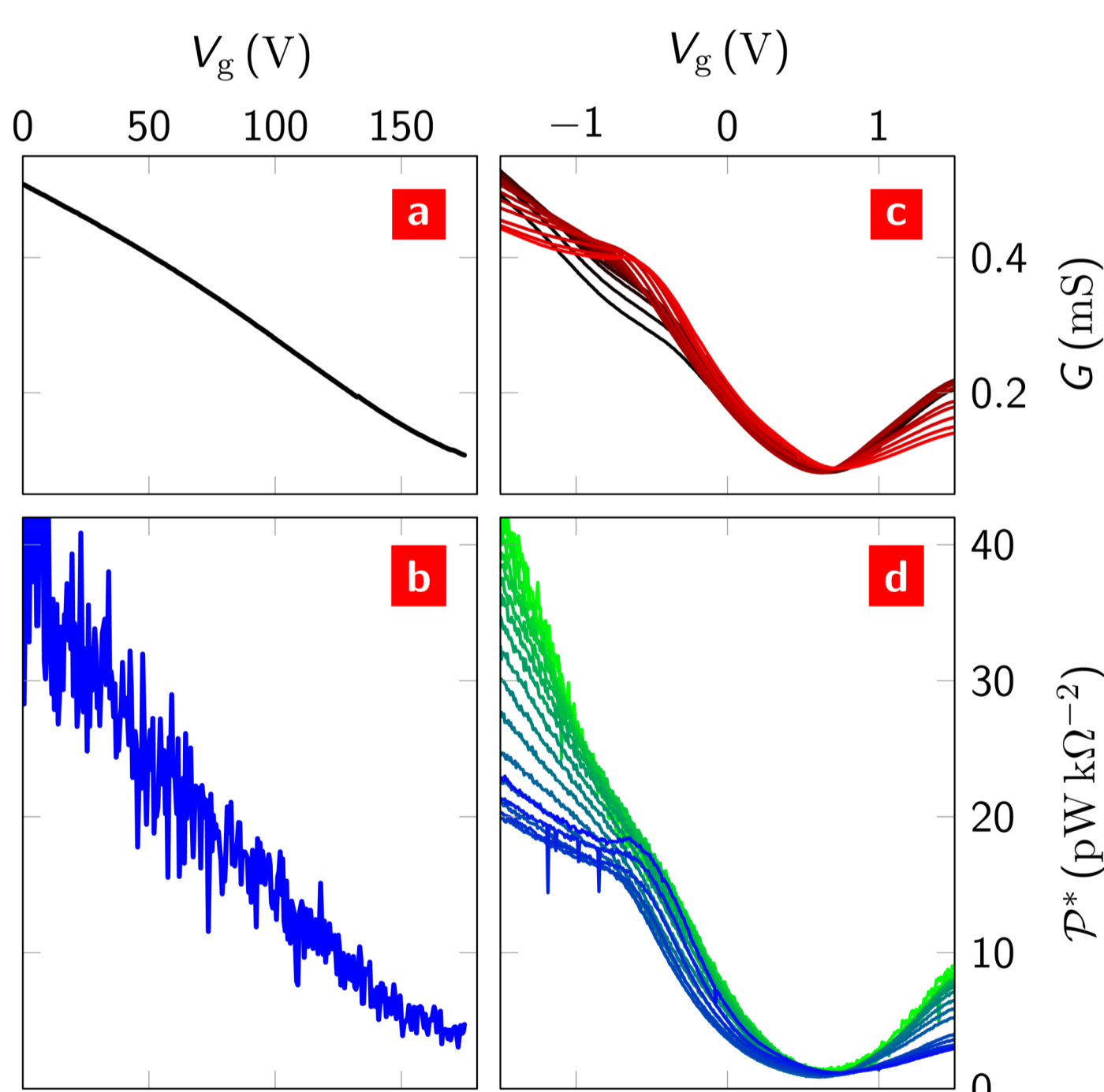
- The bottom blue group are spectra from back-gated FETs; the middle green group are spectra from top-gated FETs; the top red group are spectra from the top-gated FETs before the gate was added.
- Dashed lines are fits to Eqn. 1.
- The inset shows a typical response to a bias (red) at $f=f_1$; the response (black) is at $f_2=2f_1$.

Field-effect control

As conductance in a graphene FET is gate voltage dependent, so too is the sound output for a given bias voltage. Here we compare these dependences, the sound shown as the bias-normalised sound power

$$\mathcal{P}^* \approx \frac{2\pi}{\rho_a v_a} \left(\frac{\delta p}{V^2} \right)^2$$

- The conductance of a back-gated FET as a function of gate voltage, V_g .
- The bias-normalised sound power over the same gate voltage range at $f=20$ kHz.
- The conductance of a top-gated FET for different source powers from 0.05W (black) to 0.5W (red).
- Sound power as a function of top-gate voltage measured at $f=20$ kHz for different source powers from 0.05W (green) to 0.5W (blue).

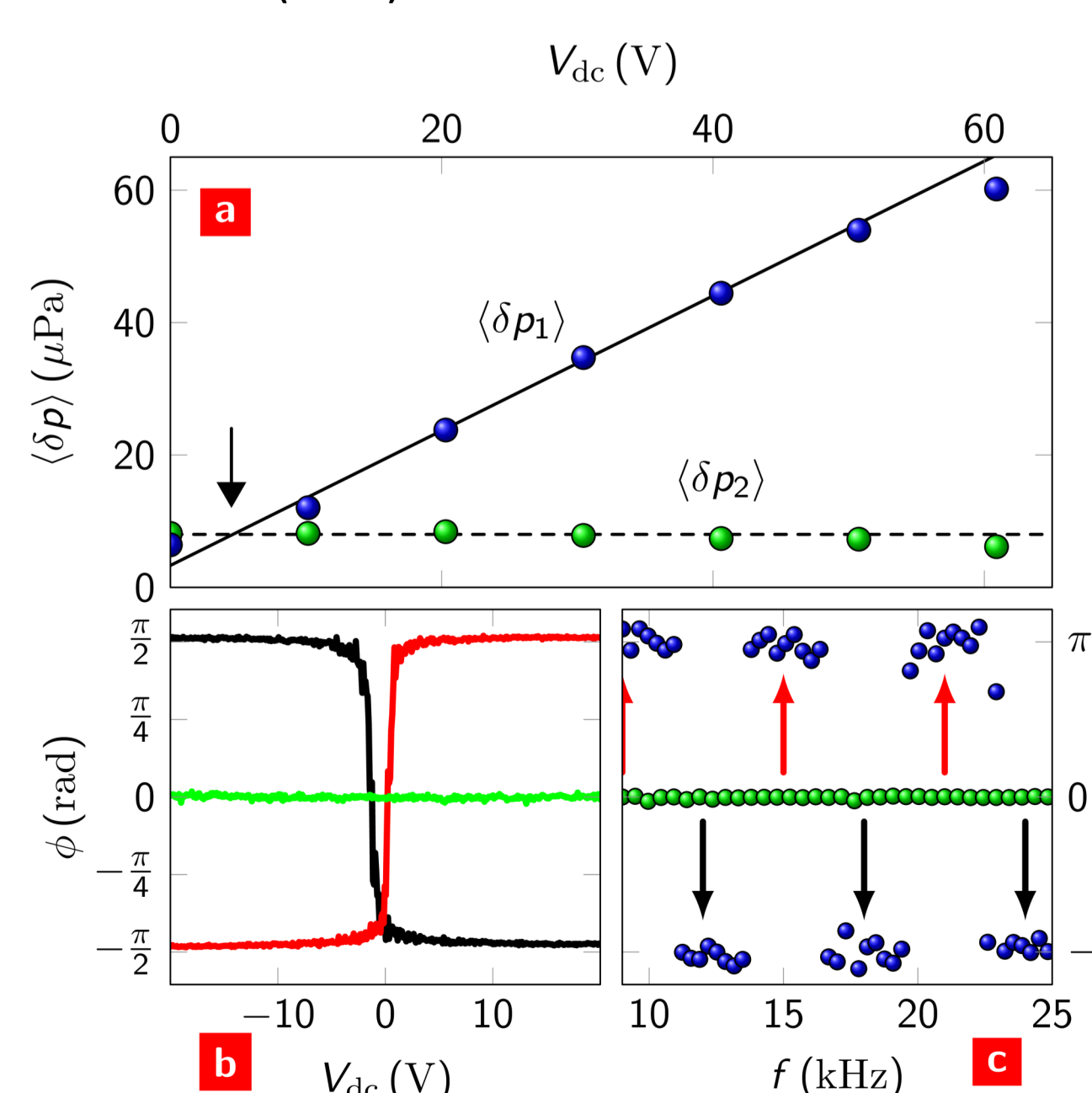


Bias-controlled polyphony

In general, the transistor channel bias can have both ac and dc components. When both are present, this generates an additional sound component at the first harmonic

$$\delta p_1 \propto GV_{ac}V_{dc}$$

- Sound pressure measured from a back-gated FET at the 1st (blue) and 2nd (green) harmonics of the source frequency as a function of dc bias.
- Phase of the 1st (black at 12kHz; red at 15kHz) and 2nd (green) harmonic response with respect to the ac source.
- The phase difference between positive and negative dc bias phase values of the 1st (blue) and 2nd (green) harmonic responses. The arrows indicate the switching events seen in (b).



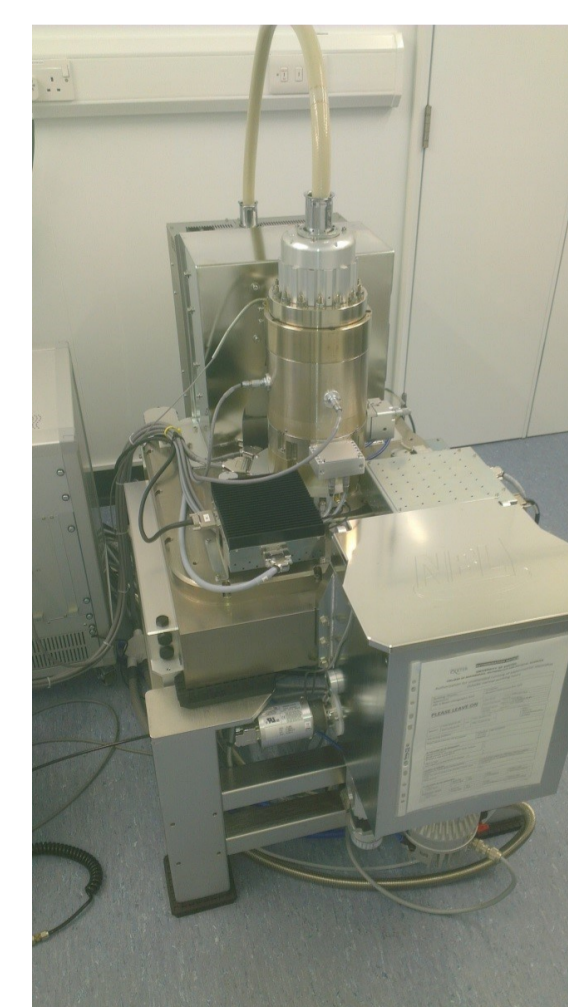
4. Conclusions

- Sound was shown to be produced by a thermoacoustic generation mechanism in gated graphene field-effect transistors. Its magnitude is defined by the material parameters of the device, the source power and frequency.
- The sound power output could be tuned over an order of magnitude by an applied gate voltage as a direct result of the dependence of the channel conductance on this voltage.
- For an ac channel bias, sound occurs only at the second harmonic of the source frequency. If a dc bias is also applied, generation occurs at both the first and second harmonics. The magnitude of the first harmonic increases linearly with dc bias.
- This linear dependence on dc bias causes the phase of the sound to switch when the polarity of the dc bias changes. The switch always has a magnitude of π radians, but its direction is frequency dependent.

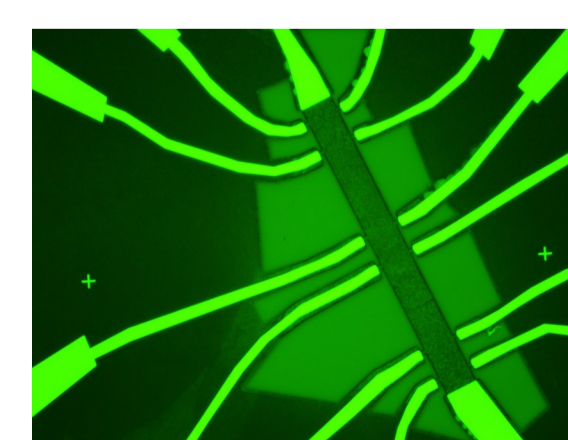
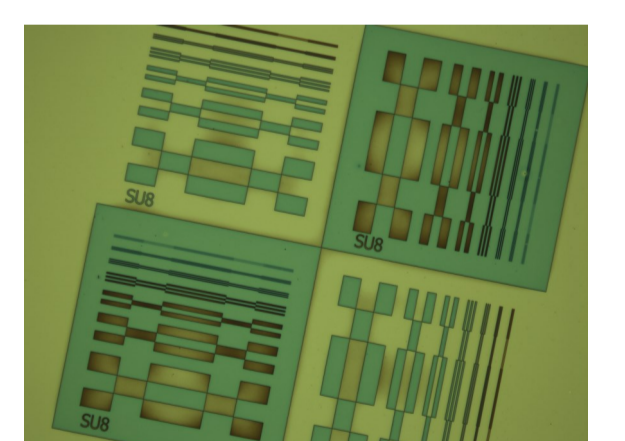
We would like to thank Thales (UK) for technical and financial support



Centre for Graphene Science at Exeter



- The centre has several clean rooms covering a total area of 150 m², housing lithography, etching, dicing and deposition systems for nanofabrication.
- Nanobeam NB4, a state-of-the-art 30kV to 100kV dedicated electron beam lithography tool, capable of producing 10nm lines ($\pm 15\%$) across a 250 μ m field using a 2nA beam.



- Durham Magneto Optics Laserwriter ML2. 405nm laser diode with optics to produce nominal spot sizes of 0.6, 1.0 and 5 μ m and up to 180mm²min⁻¹ writing speed.



- Other facilities include a HHV thermal evaporator, Loadpoint MicroAce dicer and a Kurt J Lesker e-beam evaporator. We have worked successfully with commercial and academic partners and are keen to continue with further projects and collaborations. For more information please scan the QR code or contact Mark Heath (email above)



[1] A. S. Price, S. M. Hornett, A. V. Shytov, E. Hendry and D. W. Horsell, Phys. Rev. B **85**, 161411 (2012); [2] J. W. Suk, K. Kirk, Y. Hao, N. A. Hall and R. S. Ruoff, Advanced Materials **24**, 6342 (2012); [3] H. Tian, C. Li, M. A. Mohammad, Y.-L. Cui, W.-T. Mi, Y. Yang, D. Xie and T.-L. Ren, ACS Nano **8**, 5883 (2014); [4] M. Daschewski, R. Boehm, J. Prager, M. Kreutzbruck and A. Harrer, J. App. Phys. **114**, 114903 (2013).